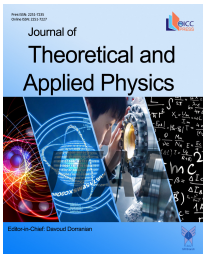

Volume 18, Issue 6, 182477 (1-10)

Journal of Theoretical and Applied Physics (JTAP)

https://dx.doi.org/10.57647/j.jtap.2024.1806.77

Study of compressed air pressure on the properties of coatings obtained by supersonic metallization

Bauyrzhan Rakhadilov[1,2], Aibek Shynarbek[1,4,*], Rinat Kusainov[1], Dauir Kakimzhanov[1,2,3], Kuanysh Ormanbekov[1], Ainur Zhassulan[1]

[1]*Shakarim University NJSC, Engineering Center SC, Semey, Kazakhstan.*
[2]*Plasma Science LLP, Ust-Kamenogorsk, Kazakhstan.*
[3]*INNOTECH MASH Engineering Center, Ust-Kamenogorsk, Kazakhstan.*
[4]*Engineering company MetPro LLP, Semey, Kazakhstan.*

[*]**Corresponding author:** shinarbekov16@gmail.com

Original Research

Received:
13 September 2024
Revised:
21 October 2024
Accepted:
4 November 2024
Published online:
30 December 2024

Abstract:

The wear and degradation of machine parts significantly impact industrial efficiency, leading to material loss and increased maintenance costs. Supersonic arc metallization (SAM) is a promising method to improve the surface properties of components by enhancing wear and corrosion resistance. This study aims to optimize the SAM process, particularly compressed air pressure, to improve the mechanical and tribological properties of 30KhGSA steel coatings. 30KhGSA steel wire was used to coat grade 45 steel samples. The effect of varying compressed air pressure was examined through tests on coating porosity, roughness, hardness, corrosion resistance, and adhesion strength. X-ray diffraction (XRD) and scanning electron microscopy (SEM) were used for microstructural analysis. Increasing air pressure led to denser coatings with lower porosity and reduced surface roughness. XRD confirmed the presence of iron oxide phases that contribute to increased hardness. Coatings produced at 9 atm displayed superior wear and corrosion resistance, with the highest hardness (331 HV) and lowest friction coefficient. Corrosion tests showed improved resistance due to lower porosity and protective oxide layers. Optimizing compressed air pressure during SAM significantly improves the wear, corrosion resistance, and adhesion strength of 30KhGSA steel coatings, offering enhanced durability for industrial applications.

Keywords: Supersonic electric arc metallization; Compressed air pressure; Coatings; Wear resistance; Corrosion resistance; Hardness; Porosity

1. Introduction

The wear and deterioration of machine parts and metal structures remain critical challenges in numerous industrial applications, leading to significant material losses, estimated at approximately 35% of the total mass of components in operation [1, 2]. This degradation negatively impacts system efficiency, reliability, and operational costs, particularly in industries such as automotive, energy, and heavy machinery, where equipment operates under high mechanical loads and in harsh environments [3, 4]. To mitigate these effects, improving the surface properties of materials—such as wear resistance, corrosion resistance, and durability—has become a key focus in extending the service life of components. Recent studies have confirmed that advanced surface engineering techniques, particularly thermal spraying methods, can significantly enhance material performance without compromising the integrity of underlying structures [5–8]. Among the various thermal spray methods, electric arc metallization (EAM) has emerged as a cost-effective and efficient solution for applying protective coatings [9, 10]. This method utilizes a high-velocity gas jet to melt and spray materials onto surfaces, forming durable coatings with minimal thermal deformation of the substrate [11, 12]. Electric arc metallization is particularly advantageous due to its

lower operational costs and high thermal efficiency, with studies showing that EAM coatings can be $4-10$ times more economical than other thermal spray methods, while still providing strong performance characteristics [13, 14]. Moreover, the ease of maintaining EAM equipment and its flexibility in applying various materials make it a valuable tool in industries that require enhanced component durability, such as automotive manufacturing, oil and gas, and aerospace sectors [15–18].

The performance of coatings applied via electric arc metallization is highly dependent on process parameters, including the material feed rate, voltage, current, air pressure, and spray distance. These factors directly influence the microstructure of the coating, particularly its porosity, hardness, and adhesion to the substrate [19–23]. Recent studies have highlighted the importance of optimizing these parameters to improve the mechanical and tribological properties of the coatings, especially in applications subjected to high wear and corrosion [24–29]. Specifically, compressed air pressure plays a pivotal role in controlling the size and distribution of particles during the napylene process, which in turn affects the coating's density and ability to resist wear [30–32]. However, despite these advancements, there is still a lack of detailed studies on how variations in air pressure during EAM impact the tribological and corrosion resistance properties of 30KhGSA steel coatings [33–38].

This study aims to address this gap by investigating the effect of compressed air pressure during electric arc metallization on the properties of 30KhGSA steel coatings. By optimizing the air pressure parameter, this research seeks to improve the wear resistance, corrosion resistance, and overall performance of these coatings, thereby extending their potential use in industries that demand high-performance components. The findings are expected to contribute to the broader field of surface engineering by offering insights into how process optimization can lead to better material properties, ultimately improving the reliability and durability of critical industrial components.

2. Materials and methods

Steel wire grade 30 KhGSA, with a diameter of 1.6 mm, was used for coating. The coatings were applied to samples of grade 45 steel, which were shaped as quarter-disk segments with a diameter of 65 mm and a thickness of 10 mm. The samples were made from grade 45 steel rods in accordance with GOST 1050-2013. The choice of steel 45 is due to its wide use in the production of various parts, such as gears and crankshafts, which are commonly used in different sectors of mechanical engineering.

Before the electric arc metallization process, the samples underwent mechanical preparation, which included grinding and treatment with quartz sand. After sandblasting, the surface roughness of the samples was measured at 2.3 μm. The coatings were applied using a supersonic electric arc metallizer SX-600. Figure 1 provides a general view and schematic of this unit. The SX-600 consists of a power supply, supersonic arc atomizer, control system, and compressed air system. The parameters of the electric arc metallization process are provided in Table 1.

An X'PertPRO X-ray diffractometer utilizing Cu-Kα radiation ($\lambda = 1.5406$ Å) was employed to analyze the phase composition of the coatings. The diffraction patterns were examined using the HighScore program over an angular range of $20-90°$, with a step size of 0.02° and a counting time of 0.5 seconds per step.

The coatings' porosity was assessed using the ImageJ soft-

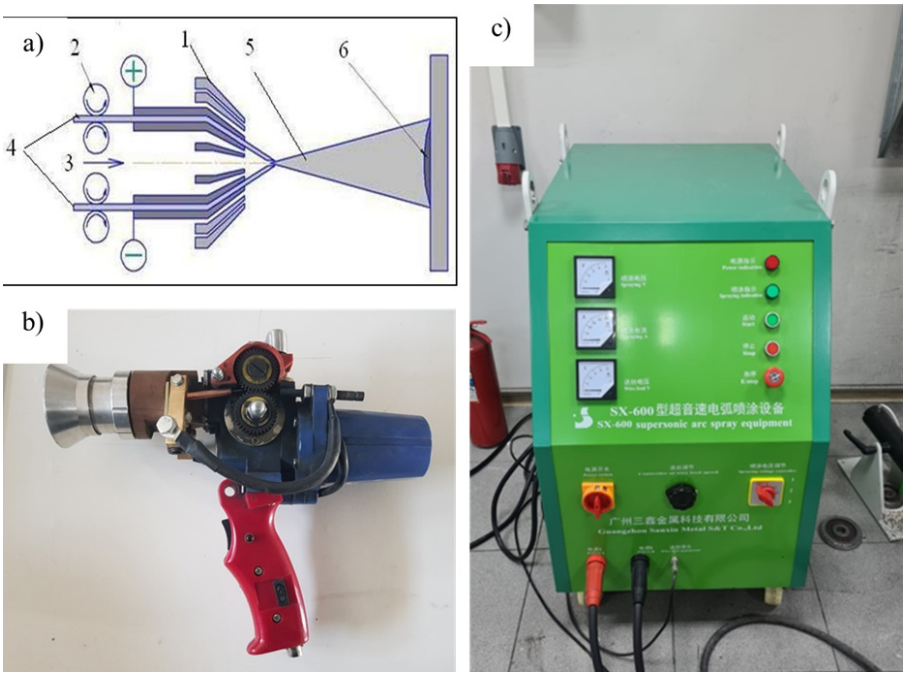

Figure 1. (a) Technological scheme of SX-600 (1 - metallizer body; 2 - wire feeding mechanism; 3 - air supply channel; 4 - electrode wires; 5 - electric arc with sprayed wire particles; 6 - sprayed coating) (b) appearance of the gun (c) appearance of the source.

Table 1. Spraying parameters.

Sample	Voltage (V)	Current (A)	Wire feed speed (cm/s)	Compressed air pressure (atm)	Spraying distance (mm)	Spraying time (s)
No.1	42	200	8	7	15	15
No.2				8		
No.3				9		

ware [39] on cross-sectional images obtained from a JSM-6390 LV JEOL scanning electron microscope. Roughness measurements were conducted using an Anytester HY2300 profilometer. The microhardness of the coatings was evaluated on the cross-section using a Vickers HLV-1DT microhardness tester, applying an indenter load of 0.2 N for a duration of 10 seconds.

Tribological properties were investigated using an Anton Paar TRB3 tribometer, with the sample positioned such that the coating surface was perpendicular to the trajectory of a 3 mm diameter ball made of 100X6 steel (equivalent to ShX15), attached to the end of a rod. The wear surface's radius of curvature was adjusted using a displacement sensor, while a friction compensation sensor measured the friction coefficient over time. The experiments were conducted in open air under a load of 10 N and a speed of 5 cm/s, with the wear surface radius of curvature set to 1.5 mm and a friction path length of 100 mm. Prior to the tribological tests, all samples were ground using a grinding machine with 240P sandpaper. The tribological characteristics of the coatings were evaluated based on wear intensity and the friction coefficient. The adhesion strength of the coatings was tested using the pin method [40]. This method involves applying a load that tears the coating away from the substrate, and the force required for detachment is recorded. The adhesion strength is determined by the following relationship:

$$\sigma_{ad} = \frac{P}{F} \tag{1}$$

where P is the breaking force.

To assess the adhesive strength using the pin method, samples were prepared (see Fig. 2) consisting of a pin and a substrate, with a gripping device that included a hole and a fastening element to secure the pin. The sample featured a washer with a hole where the pin was installed, ensuring that its end surface was flush with the outer plane of the washer. The coating was applied to the shared surface of the pin's end and the washer. To prevent the pin from dislodging during the spraying process, it was secured with a screw. The pin was then pulled from the base using a universal tensile testing machine (WDW-100 kN). The adhesion strength was calculated by dividing the maximum force at which the coating detached by the area of the pin's end surface.

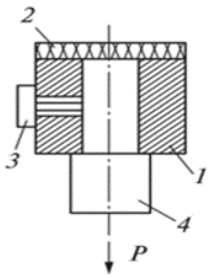

Figure 2. Schematic diagram of the manufactured sample for testing coating adhesion strength using the pin method: 1 - substrate (45 steel); 2 - coating; 3 - retainer; 4 - pin.

The corrosion resistance of the coatings was evaluated using an electrolytic cell equipped with a Potentiostat cs300m. Measurements were conducted in a 3.5% NaCl solution using a three-electrode setup: the working electrode was the EAM-deposited coating on grade 45 steel, the reference electrode was a silver-silver chloride electrode, and the auxiliary electrode was a platinum electrode.

3. Results

3.1 Study of porosity and morphology of coatings

Figure 3 presents scanning electron microscope (SEM) images of cross-sections of coatings produced by supersonic arc spraying. As shown in Figures 3 (a, b, c), the coating thickness varies depending on the parameters used. Increasing the compressed air pressure appears to reduce the atomization efficiency, likely due to a decrease in particle size. The specific coating thickness values are provided in Table 2. It is also evident that higher compressed air pressure results in denser coatings with reduced porosity.

Figures 3 (d, e, f) display images at 5000x magnification used to analyze porosity with the ImageJ software package. These images demonstrate that increasing compressed air pressure leads to a decrease in porosity, as reflected by a reduction in both average pore size and overall porosity percentage. The porosity values are provided in Table 2.

3.2 Roughness test results

Figure 4 illustrates the surface roughness of coatings following supersonic arc metallization (SAM). The roughness was evaluated using the Ra parameter, which represents the arithmetic mean deviation of the surface profile. The images indicate that higher compressed air pressure results in reduced roughness. For example, the Ra values are 20.054 μm for sample No. 1, 19.16 μm for sample No. 2, and 14.358 μm for sample No. 3.

As compressed air pressure increases, the kinetic energy of the particles also rises, leading to more forceful impacts on the substrate surface. This results in a denser and more uniform material distribution. The high velocity of the par-

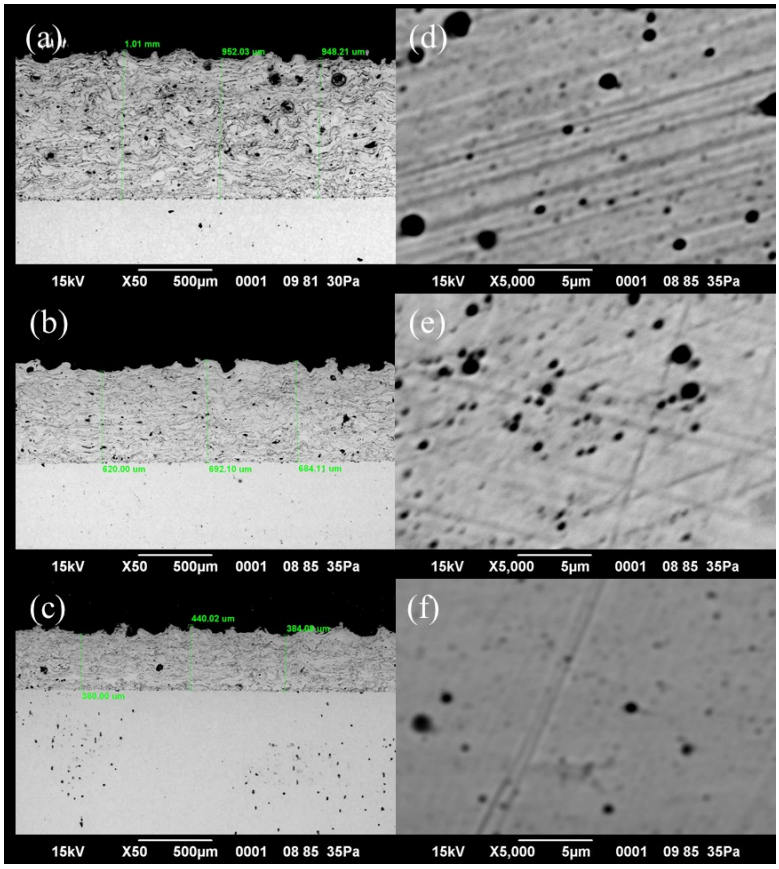

Figure 3. SEM images of cross sections of samples with magnification ×50: (a) No.1; (b) No.2; (c) No.3 and images of coatings with magnification ×5000: (d) No.1; (e) No.2; (f) No.3.

Table 2. Coating thickness and porosity value.

Sample	Coating thickness (μm)	Average pore size (μm)	Percentage of porosity (%)
No.1	966.78 ± 22.21	0.380	2.901
No.2	665.4 ± 30.27	0.255	2.657
No.3	401.36 ± 25.77	0.131	2.206

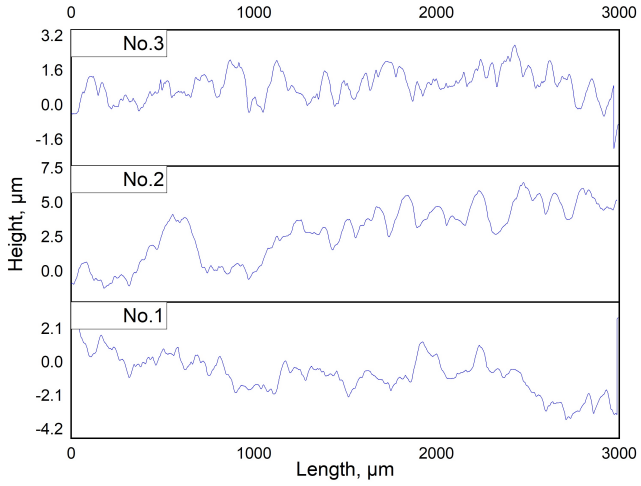

Figure 4. Results of coating roughness assessment.

ticles upon striking the substrate enhances the sintering and merging of the particles with each other and with the substrate, thereby decreasing the number of microvoids and surface irregularities, which in turn lowers the roughness. Additionally, increased air pressure enhances material atomization, promoting a more uniform particle distribution across the surface and contributing to the formation of a smoother coating with fewer height variations [41–44].

3.3 X-ray diffraction analysis

Figure 5 presents the results of X-ray diffraction analysis, confirming the presence of iron oxide (FeO) and alpha iron (α-Fe) in the coatings. After being sprayed onto the substrate, the molten particles cool rapidly and solidify. This rapid cooling helps preserve the oxide phases that formed during the spraying process. FeO can stabilize on the coating surface during rapid cooling, as its further transformation into other oxides (e.g., Fe_2O_3 or Fe_3O_4) may be inhibited. The figure shows that as compressed air pressure increases, the intensity of the FeO peaks in the diffraction patterns also increases, highlighting the influence of pressure on the phase composition of the coatings [45–48]. Additionally, at higher compressed air pressure, a decrease in the intensity of the alpha iron peaks is observed, accompanied by an increase in the intensity of the FeO peaks. The presence of solid iron oxide particles in the metal matrix acts as a dispersed hardener. These particles hinder the movement of dislocations in the crystal lattice, thereby increasing the hardness of the material [49, 50].

3.4 Study of mechanical and tribological properties of coatings

Figure 6 (a) indicates that the hardness of coatings produced through supersonic arc metallization exceeds that of Steel 45. As the compressed air pressure increases, the hardness of the coatings also rises. The 30KhGSA steel wire used for spraying has a hardness of 286 HV, which is higher than that of steel 45 at 201 HV. Interestingly, the hardness of the coatings surpasses that of the original wire. Sample No.1, processed at a compressed air pressure of 7 atm, shows a hardness of 309.33 ± 13.89 HV; Sample No.2, at 8 atm, has a hardness of 314.2 ± 12.1 HV; and Sample No.3, at 9 atm, reaches 331 ± 10.32 HV.

The increase in coating hardness compared to the original 30 KhGSA wire after supersonic arc metallization is attributed to the rapid cooling of metal particles upon contact with the substrate, caused by the cold jet of compressed air, which leads to their instantaneous solidification [51, 52]. The rise in hardness with higher compressed air pressure is linked to increased coating density resulting from greater kinetic energy. The density of the sprayed metal is influenced by the particle velocity before impact and their size; smaller particles contribute to higher hardness, and dispersion improves with increased compressed air pressure.

Figure 6 (b) presents the results for the friction coefficient, showing the following values: Steel 45 – 0.472; Sample No.1 – 0.538; Sample No.2 – 0.528; Sample No.3 – 0.523. These findings indicate that the wear resistance of the coatings can be enhanced by increasing the compressed air pressure. As the compressed air pressure rises, the average pore size decreases, contributing to improved antifriction properties of the coatings.

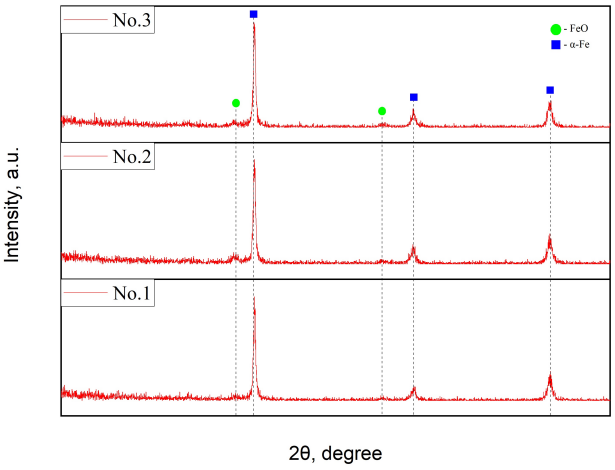

Figure 5. Results of X-ray structural analysis of the obtained coatings.

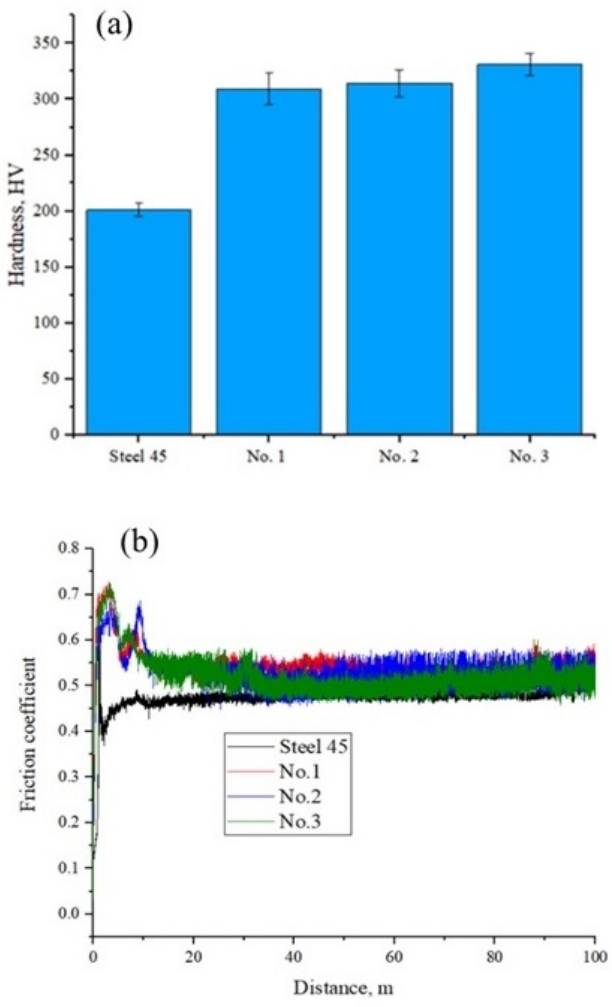

Figure 6. Results of mechanical and tribological tests of grade 45 steel and obtained coatings: (a) hardness (b) friction coefficient.

In the tribological tests, as shown in Figure 7, the wear morphology of the coated samples reveals wear marks and micro-scratches along the friction path. With increasing compressed air pressure during the spraying process, the porosity decreases, leading to denser and more compact coatings. This results in a noticeable improvement in wear behavior, with Sample No.1 (7 atm) showing deeper and more pronounced wear marks compared to Samples No.2 (8 atm) and No.3 (9 atm), which exhibit smoother wear tracks. The average wear track diameter supports this observation: Sample No.1 has the largest wear track (average D = 640.99 ± 14.47 μm), followed by Sample No.2 (average D = 602.67 ± 12.98 μm) and Sample No.3 (average D = 560.98 ± 15.68 μm).

The reduction in pore size as the compressed air pressure increases enhances the wear resistance of the coatings, leading to a denser structure that better withstands frictional forces. This correlation between lower porosity and improved tribological properties highlights the effectiveness of optimizing the air pressure during the supersonic arc spraying process. Despite the presence of wear marks, the coatings maintain a consistent friction profile, with increased air pressure contributing to better wear resistance through reduced porosity and enhanced surface integrity.

3.5 Corrosion resistance research results

The corrosion resistance of coatings produced by supersonic arc metallization (SAM) is closely tied to the porosity and density of the coatings. As demonstrated by the results presented in Table 3, the coatings sprayed at a compressed air pressure of 9 atm exhibit the lowest corrosion current density and, consequently, the lowest corrosion rate. This enhanced performance can be attributed to the densification of the coating structure under higher pressures. As compressed air pressure increases, the kinetic energy of the molten particles also increases, allowing them to strike

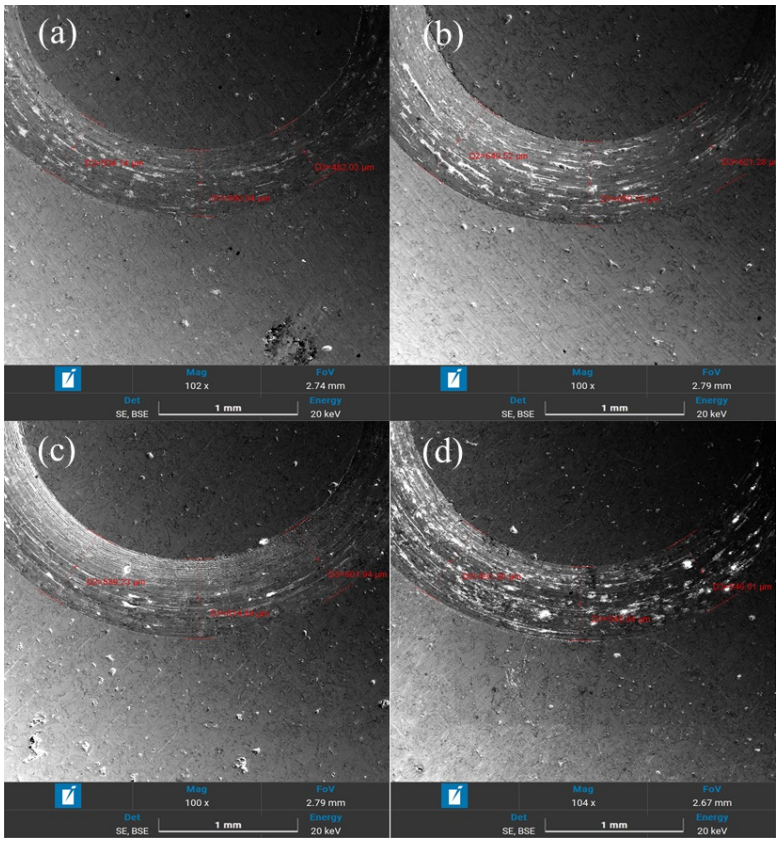

Figure 7. SEM images of the coating morphology after tribological tests: (a) steel 45, (b) No.1, (c) No.2, (d) No.3.

Table 3. Results of calculation of corrosion parameters of samples.

Sample	Corrosion current Iκ, $(\mu A/cm)^2$	Free corrosion potential Eκ, (V)	Corrosion rate (mm/year)
Steel 45	1.6481E-05	−0.45487	0.19334
No.1	6.5093E-0,6	−0.3942	0.076362
No.2	5.3661E-06	−0.36523	0.062951
No.3	1.8995E-06	−0.39675	0.022284

the substrate with greater force. This results in improved particle sintering, which reduces the number of microvoids and pores within the coating.

Porosity plays a crucial role in corrosion behavior, as it can act as a pathway for aggressive ions and corrosive media to penetrate the coating and reach the substrate. A decrease in porosity, as observed in coatings produced at higher air pressures, limits this penetration, thereby enhancing the protective properties of the coating. Studies such as those referenced in [53] confirm that reducing porosity correlates directly with improved corrosion resistance, as a denser coating provides a more effective barrier to environmental degradation.

The Tafel curves presented in Figure 8 further illustrate this relationship. The electrochemical behavior of the coatings shows a clear shift in both corrosion potential and corrosion current density, with the most significant improvements observed at 9 atm. Higher air pressure leads to a greater concentration of FeO phases, which may further enhance corrosion resistance by forming a protective oxide layer on the coating surface. This oxide layer acts as a passivation barrier, reducing the reactivity of the underlying metal and slowing down the rate of corrosion.

Additionally, coatings produced at lower air pressures, such as 7 and 8 atm, still display improved corrosion resistance compared to the original uncoated sample. However, the presence of more significant porosity in these coatings limits their performance relative to the higher-pressure coatings. The overall trend confirms that the porosity reduction with increased pressure is a key factor in achieving better corrosion resistance, as it directly influences the coating's ability to withstand environmental exposure.

Therefore, by optimizing the compressed air pressure during supersonic arc metallization, it is possible to significantly improve the corrosion resistance of steel coatings. This is achieved through both physical densification and the formation of beneficial oxide phases, which together enhance the durability and protective characteristics of the coatings in corrosive environments.

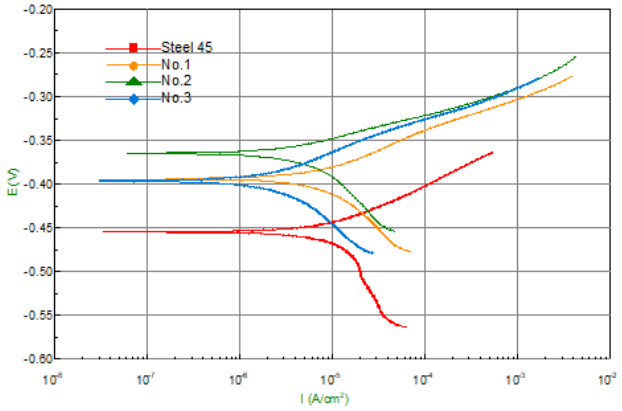

Figure 8. Diagram of the results of measurements of electrochemical corrosion of the obtained coatings and grade 45 steel.

Table 4. Test results of adhesion strength of coatings.

Sample	Coating bond strength (MPa)
No.1	15.43 ± 2.11
No.2	18.55 ± 1.65
No.3	22.32 ± 0.95

3.6 Results of a study of the adhesion strength of coatings

The results of the adhesion strength tests showed that the coating on Sample 3, obtained with the parameters of supersonic arc metallization (SAM) at 9 atm, exhibited the highest adhesion strength. This is likely due to the fact that higher pressure contributed to a significant acceleration of the molten particles of the 30 KhGSA surfacing wire, increasing their kinetic energy and improving their bonding with the substrate. The data on adhesion strength test results are provided in Table 4. It can also be observed that a lower mechanical force of 18 and 15 MPa, respectively, was required to break the coatings on samples 1 and 2. This supports the conclusion that increasing pressure during SAM enhances the adhesive properties of the 30 KhGSA coating. Additionally, it was noted that a distinct boundary was observed when the coatings separated from the substrate, indicating strong cohesive qualities in all samples.

4. Conclusion

Increasing compressed air pressure during supersonic arc metallization (SAM) significantly improves the quality of coatings by reducing porosity and enhancing density. SEM analysis shows that higher pressure leads to more effective atomization, resulting in a smoother and more compact surface. This also reduces surface roughness, as higher kinetic energy ensures better material distribution and compaction.

X-ray diffraction reveals that increased pressure contributes to higher concentrations of iron oxide (FeO), which strengthens the coating through dispersed hardening. This, along with the rapid cooling of particles during SAM, results in greater hardness, exceeding that of the original wire material.

The coatings also show improved wear resistance and lower friction coefficients due to reduced porosity, contributing to enhanced antifriction properties. Additionally, corrosion resistance is significantly increased at higher pressures, as reduced porosity limits the penetration of corrosive agents. Finally, adhesion strength improves with higher pressure, with the best results observed at 9 atm. The elevated particle velocity and better bonding with the substrate result in stronger, more durable coatings. These improvements make SAM an optimal technique for producing high-performance coatings, especially for applications requiring wear resistance and longevity, such as in crankshaft restoration.

Authors contributions
Bauyrzhan Rakhadilov contributed to the conception, setup design, data analysis, and finalization of the paper. Aibek Shynarbek was responsible for the setup design, experiment, data analysis, draft writing, and finalization of the paper. Rinat Kusainov contributed to the experiment and draft writing. Daur Kakimzhanov was involved in the setup design, data analysis, and experiment. Kuanysh Ormanbekov contributed to the conception and data analysis. Ainur Zhassulan was responsible for the setup design and finalization of the paper. Each author made substantial contributions to the research, analysis, and writing processes, ensuring the quality and integrity of the final manuscript.

Funding
This research has been funded by the Science Committee of the Ministry of Science and Higher Education of the Republic of Kazakhstan (Grant No AP14871373).

Availability of data and materials
The data that support the findings of this study are available on request from the corresponding author.

Conflict of interests
The author declare that they have no known competing financial interests or personal relationships that could have appeared to influence the work reported in this paper.

References

[1] J. Krmela, T. P. Hovorun, K. V. Berladir, and A. Y. Artiukhov. "Increasing the structural strength of corrosion-resistant steel for elastic components of diaphragm compressor.". *Manufacturing Technology*, **21**:207–213, 2021. DOI: https://doi.org/10.21062/mft.2021.034.

[2] A. A. Ivanov and T. N. Oskolkova. "Heat treatment of steel 30KhGSA on the specialized equipment. ". *IOP Conference Series: Materials Science and Engineering*, **411**:012034, 2018. DOI: https://doi.org/10.1088/1757-899X/411/1/012034.

[3] S. Singh, C. C. Berndt, R. K. Singh Raman, H. Singh, and A. S. Ang. "Applications and developments of thermal spray coatings for the iron and steel industry. ". *Materials*, **16**:516, 2023. DOI: https://doi.org/10.1088/1757-899X/233/1/012027.

[4] P. V. Kosenko. "The applicability of existing renovation methods in technology of screw compressors repairing. ". *IOP Conference Series: Materials Science and Engineering*, **233**:012027, 2017. DOI: https://doi.org/10.1088/1757-899X/233/1/012027.

[5] E. J. Gildersleeve and R. Vaßen. "Thermally sprayed functional coatings and multilayers: a selection of historical applications and potential pathways for future innovation. ". *Journal of Thermal Spray Technology*, **32**:778–817, 2023. DOI: https://doi.org/10.1007/s11666-023-01587-1.

[6] C. U. Hardwicke and Y. C. Lau. "Advances in thermal spray coatings for gas turbines and energy generation: a review. ". *Journal of Thermal Spray Technology*, **22**: 564–576, 2013. DOI: https://doi.org/10.1007/s11666-013-9904-0.

[7] D. Tejero-Martin, M. Rezvani Rad, A. McDonald, and T. Hussain. "Beyond traditional coatings: a review on thermal-sprayed functional and smart coatings. ". *Journal of Thermal Spray Technology*, **28**:598–644, 2019. DOI: https://doi.org/10.1007/s11666-019-00857-1.

[8] S. J. Dapkunas. "Conference Report: NIST-INDUSTRY WORKSHOP ON THERMAL SPRAY COATINGS RESEARCH Gaithersburg, MD July 20, 1992.". *Journal of Research of the National Institute of Standards and Technology*, **98**:383, 1993. DOI: https://doi.org/10.6028/jres.098.030.

[9] G. R. Bell. "Thermal spraying for cost reduction and efficiency. ". *Materials and Design*, **4**:783–790, 1983.

[10] P. Vuoristo and P. Nylén. "Industrial and research activities in thermal spray technology in the Nordic region of Europe. ". *Journal of Thermal Spray Technology*, **16**:466–471, 2007. DOI: https://doi.org/10.1007/s11666-007-9136-2.

[11] S. Wang, X. Cui, G. Jin, Y. Liu, X. Wen, W. Zheng, and S. Wan. "Study on microstructure and wear resistance of laser cladding TiAlZrVNiX high entropy alloy coating based on Laves phase modulation. ". *Surface and Coatings Technology*, **490**:131197, 2024. DOI: https://doi.org/10.1016/j.surfcoat.2024.131197.

[12] J. Oberste-Berghaus, M. Aghasibeig, A. Burgess, P. Khamsepour, C. Moreau, and A. Dolatabadi. "Exploring miniaturized HVOF systems for the deposition of Ti-6Al-4V. ". *Journal of Thermal Spray Technology*, **2**:760–772, 2023. DOI: https://doi.org/10.1007/s11666-023-01531-3.

[13] C. M. Sample, V. K. Champagne, A. T. Nardi, and D. A. Lados. "Factors governing static properties and fatigue, fatigue crack growth, and fracture mechanisms in cold spray alloys and coatings/repairs: A review. ". *Additive Manufacturing*, **36**:101371, 2020. DOI: https://doi.org/10.1016/j.addma.2020.101371.

[14] N. Espallargas. "Future development of thermal spray coatings: types, designs, manufacture and applications. ". *Woodhead Publishing*, :1–13, 2015. DOI: https://doi.org/10.1016/B978-0-85709-769-9.00001-4.

[15] S. Celotto, J. Pattison, J. S. Ho, A. N. Johnson, and W. ÓNeill. "The cold spray materials deposition process. The economics of the cold spray process.". *Woodhead Publishing*, :72–101, 2007. DOI: https://doi.org/10.1533/9781845693787.1.72.

[16] R. C. Tucker Jr. "Thermal spray technology. ". *ASM HANDBOOK*, , 2013. DOI: https://doi.org/10.31399/asm.hb.v05a.a0005748.

[17] A. Vardelle, C. Moreau, J. Akedo, H. Ashrafizadeh, C. C. Berndt, J. O. Berghaus, and P. Vuoristo. "The 2016 thermal spray roadmap. ". *Journal of Thermal Spray Technology*, **25**:1376–1440, 2016. DOI: https://doi.org/10.1007/s11666-016-0473-x.

[18] M. R. Dorfman. "Thermal spray coatings. In Handbook of environmental degradation of materials.". *William Andrew Publishing*, :469–488, 2018. DOI: https://doi.org/10.1016/B978-0-323-52472-8.00023-X.

[19] Y. S. Korobov. "Efficiency of using activated arc metallising for the deposition of protective coatings. ". *Welding International*, **19**:580–582, 2005. DOI: https://doi.org/10.1533/wint.2005.3483.

[20] N. Parkansky, R. L. Boxman, and S. Goldsmith. "Development and application of pulsed-air-arc deposition. ". *Surface and Coatings Technology*, **61**: 268–273, 1993. DOI: https://doi.org/10.1016/0257-8972(93)90237-I.

[21] H. D. Steffens, Z. Babiak, and M. Wewel. "Recent developments in arc spraying.". *IEEE Transactions on Plasma Science*, **18**:974–979, 1990. DOI: https://doi.org/10.1109/27.61512.

[22] J. S. Chen, Y. Lu, X. R. Li, and Y. M. Zhang. "Gas tungsten arc welding using an arcing wire. ". *Welding Journal*, **91**:261–269, 2012.

[23] A. Singh, V. Sharma, S. Mittal, G. Pandey, D. Mudgal, and P. Gupta. "An overview of problems and solutions for components subjected to fireside of boilers. ". *International Journal of Industrial Chemistry*, **9**:1–15, 2018. DOI: https://doi.org/10.1007/s40090-017-0133-0.

[24] Y. P. Qian, J. H. Huang, H. O. Zhang, and G. L. Wang. "Direct rapid high-temperature alloy prototyping by hybrid plasma-laser technology. ". *Journal of Materials Processing Technology*, **208**:99–104, 2008. DOI: https://doi.org/10.1016/j.jmatprotec.2007.12.116.

[25] P. K. Shrivastava, S. Pandey, and S. Dangi. "Electrical arc machining: process capabilities and current research trends. ". *Proceedings of the Institution of Mechanical Engineers, Part C: Journal of Mechanical Engineering Science*, **233**:5190–5200, 2019. DOI: https://doi.org/10.1177/09544062198461.

[26] V. Makienko, I. Romanov, P. Sokolov, A. Atenyaev, and D. Pervakov. "Research into special technological effects for formation of wear resistant coatings using mineral raw materials of the far eastern region. ". *E3S Web of Conferences; EDP Sciences*, **56**:03027, 2018. DOI: https://doi.org/10.1051/e3sconf/20185603027.

[27] V. P. Smolentsev, O. N. Fedonin, and E. V. Smolentsev. "Electroerosion formation and technology of cast iron coatings on aluminum alloys. ". *MATEC Web of Conferences; EDP Sciences*, **129**:01016, 2017. DOI: https://doi.org/10.1051/matecconf/201712901016.

[28] M. Vostřák, J. Brodský, Š. Houdková, and P. Šulcová. "Possibilities of using thermally sprayed coatings for surface treatment of rail vehicles components". *IOP Conference Series: Materials Science and Engineering*, **1178**:012065, 2021. DOI: https://doi.org/10.1088/1757-899X/1178/1/012065.

[29] J. Vetter, A. O. Eriksson, A. Reiter, V. Derflinger, and W. Kalss. "Quo vadis: Alcr-based coatings in industrial applications. ". *Coatings*, **11**:344, 2021. DOI: https://doi.org/10.3390/coatings11030344.

[30] J. Hesselbach, A. C. Böttcher, I. Kampen, G. Garnweitner, C. Schilde, and A. Kwade. "Process and formulation strategies to improve adhesion of nanoparticulate coatings on stainless steel. ". *Coatings*, **8**:156, 2018. DOI: https://doi.org/10.3390/coatings8050156.

[31] T. Häfner, B. Rothammer, J. Tenner, K. Krachenfels, M. Merklein, S. Tremmel, and M. Schmidt. "Adaption of tribological behavior of aC: H coatings for application in dry deep drawing.". *MATEC Web of Conferences*, **190**:14002, 2018. DOI: https://doi.org/10.1051/matecconf/201819014002.

[32] P. Schwarz, S. Weber, and F. Deuerler. "Influence of particle reinforcement and heat treatment on the wear resistance of inductively melted hardpaint coatings. .". *Metals*, **10**:968, 2020. DOI: https://doi.org/10.3390/met10070968.

[33] S. Slegers, M. Linzas, J. Drijkoningen, J. D'Haen, N. K. Reddy, and W. Deferme. "Surface roughness reduction of additive manufactured products by applying a functional coating using ultrasonic spray coating. ". *Coatings*, **7**:208, 2017. DOI: https://doi.org/10.3390/coatings7120208.

[34] K. Bobzin, T. Brögelmann, N. C. Kruppe, and M. Carlet. "Wear behavior and thermal stability of HPPMS (al, ti, cr, si) ON, (Al, ti, cr, si) n and (ti, al, cr, si) n coatings for cutting tools. ". *Surface and Coatings Technology*, **385**:125370, 2020. DOI: https://doi.org/10.1016/j.surfcoat.2020.125370.

[35] D. I. Shlimas, A. L. Kozlovskiy, M. E. Kaliekperov, K. K. Kadyrzhanov, and V. V. Uglov. "Study of the strength characteristics and radiation resistance of thin-film coatings based on CuX (X = Bi, Mg, Ni). ". *Eurasian Journal of Physics and Functional Materials*, **4**:234–241, 2020. DOI: https://doi.org/10.29317/ejpfm.2020040305.

[36] S. Khimukhin, K. Eremina, and H. Ri. "Nickel aluminides coatings on steel C1030 after thermal cycling. ". *Materials Today: Proceedings*, **11**:240–246, 2019. DOI: https://doi.org/10.1016/j.matpr.2018.12.137.

[37] E. N. Eremin, A. S. Losev, I. A. Ponomarev, S. A. Borodikhin, and M. N. Volochayev. "Wear resistance of steel obtained by surfacing a flux-cored wire 30N8Kh6M3STYu. ". *Journal of Physics: Conference Series*, **1546**:012060, 2020. DOI: https://doi.org/10.1088/1742-6596/1546/1/012060.

[38] M. V. Perovskaya and V. V. Shmakov. "Structure and properties of coatings based on chromium and boron carbides deposited in a relativistic electron beam.". *AIP Conference Proceedings*, **2310**, 2020. DOI: https://doi.org/10.1063/5.0034131.

[39] National Institutes of Health. "Image Processing and Data Analys is in Java. ". , 2016.

[40] I. D. Ibatullin, M. D. Karlova, and D. R. Zagidullina. " Instruments and methods for assessing the quality of coatings. ". *Izvestiya of the Samara Scientific Center of the Russian Academy of Sciences*, **18**:291–296, 2016.

[41] I. S. Bodnya and V. P. Timoshenko. "Analysis of thermal regimes of the front composite edge of a small-sized aerospace vehicle wing.". *Engineering Journal: Science and Innovation*, **9**:6, 2018.

[42] F. I. Panteleenko, M. A. Belotserkovsky, M. N. Karpets, et al. "Comparative analysis of the physico-mechanical properties of coatings applied by electric arc and hypersonic metallization methods. ". *Mechanics of Machines, Mechanisms and Materials*, **4**:48–54, 2019.

[43] E. Astrashab, M. Belotserkovsky, A. Grigorchik, et al. "Influence of spraying air pressure during high-velocity thermal spraying of high-chromium steel coating on its structure and wear resistance. ". *Mechanics of Machines, Mechanisms and Materials*, **4**:51–57, 2018.

[44] Yu. S. Borisov, N. V. Vigilyanskaya, I. A. Demyanov, et al. "Investigation of the influence of electric arc spraying modes on the structure and properties of pseudo-alloy coatings. ". *Automatic Welding*, **12**:11–17, 2013.

[45] B. Wielage, H. Pokhmurska, M. Student, et al. "Iron-based coatings arc-sprayed with cored wires for applications at elevated temperatures. ". *Surf Coat Technol*, **220**:27–35, 2013. DOI: https://doi.org/10.1016/j.surfcoat.2012.12.013.

[46] B. A. Matyushkin, V. I. Denisov, and A. A. Tolkachev. "Technological features of electric arc metallization in the agricultural sector. ". *Weld Prod*, **12**:46–50, 2016.

[47] V. N. Logachev and N. N. Litovchenko. "Electric arc metallization: ways to improve equipment and technology. ". *Proceedings of GOSNITI*, **117**:228–234, 2014.

[48] P. V. Kiryukhantsev-Korneev. "Pulsed magnetron sputtering of ceramic SHS targets as a promising technique for deposition of multifunctional coatings.". *Prot Met Phys Chem Surf*, **56**:343–357, 2020. DOI: https://doi.org/10.1134/S2070205120020124.

[49] M. Hahn, R. Theissmann, B. Gleising, et al. "Microstructural alterations within thermal spray coatings during highly loaded diesel engine tests. ". *Wear*, **267**:916–924, 2009. DOI: https://doi.org/10.1016/j.wear.2008.12.109.

[50] K. Bobzin, F. Ernst, K. Richardt, et al. "Thermal spraying of cylinder bores with the Plasma Transferred Wire Arc process. ". *Surf Coat Technol*, **202**:4438–4443, 2008. DOI: https://doi.org/10.1016/j.surfcoat.2008.04.023.

[51] R. N. Saifullin and A. P. Pavlov. "Evaluation of the adhesion strength of coatings obtained by electrocontact welding of the mesh, depending on the welding modes.". *Bulletin of Polotsk State University. Series B. Industry. Applied Sciences*, **3**:91–96, 2013.

[52] M. V. Ushakov, S. N. Kutepov, D. S. Klementyev, et al. "Influence of spraying process parameters on the physico-mechanical and corrosion properties of protective coatings. ". *Tech Sci*, **2**:584–590, 2023. DOI: https://doi.org/10.24412/2071-6168-2023-2-584-591.

[53] J. Lin, Z. Wang, P. Lin, et al. "Microstructure and corrosion resistance of iron-based coatings produced by twin-wire arc spraying. ". *J Therm Spray Technol*, **23**:333–339, 2014. DOI: https://doi.org/10.1007/s11666-014-0110-9.